Available online at www.dergipark.gov.tr

INTERNATIONAL ADVANCED RESEARCHES and ENGINEERING JOURNAL

Journal homepage: www.dergipark.gov.tr/iarej

e-ISSN: 2618-575X

International Open Access

Volume 03
Issue 03

December, 2019

Research Article

TEM characterization and synthesis of nanoparticle B_4C by high-energy milling

Hakan Gokmese [a,*], ***Bulent Bostan*** [b], ***Taha Alper Yilmaz*** [c] ***and Ufuk Tasci*** [d]

[a]*Necmettin Erbakan University, Faculty of Seydisehir Ahmet Cengiz Engineering, Konya, 42370, Turkey*
[b]*Gazi University, Faculty of Technology, Ankara, 06500, Turkey*
[c]*University of Atatürk, Faculty of Engineering, Metallurgical and Materials Engineering, Erzurum, 25240, Turkey*
[d]*University of Gazi, Technical Sciences Vocational School, Ankara, 06374, Turkey*

ARTICLE INFO

Article history:
Received 08 October 2019
Revised 24 October 2019
Accepted 05 November 2019

Keywords:
TEM
Diffraction pattern
B_4C
Nanoparticle
Synthesis

ABSTRACT

In this study, nanoparticle B_4C synthesis was carried out by high-energy milling. For this purpose, B_2O_3-C-Mg triple systems were used in the reaction stoichiometric ratios as starting materials in the experimental studies. The reduction process of B_2O_3 was performed using speks type milling device. The transformation of the ceramic phase of the nanoparticle B_4C by XRD analysis was examined. In terms of microstructural characterization of its powder shape and morphology, TEM (imaging and selected area diffraction pattern) investigations were conducted. The product synthesized by the leaching process was cleaned from MgO/B_4C impurities and the production of the nanoparticle B_4C was performed. After leaching processes, it was determined that some of the synthesized powders were below 50 nm, while others varied between the ranges of 50-350 nm. In TEM examinations of B_4C particles carried out after leaching process, it was seen that there were twin formations observed as planar error. Depending on the d values calculated by solving the TEM diffraction patterns, the planes represented by nano-sized B_4C particles were determined.

1. Introduction

It is said that the mechanochemical synthesis will be one of the most important methods in the future for the production of composite materials and it is becoming the focus of attention by the day [1]. Mechanochemical synthesis is a solid-state powder-material synthesis method involving chemical reactions at room temperature or lower temperatures following the mixture of reaction start powders [2].

The chemical reaction in question can be either during the mechanical alloying process or by the heat treatment of mechanically alloyed powders. In this process, metal powders are subjected to milling with a combination of metal powders and reactive elements to synthesize thermally stable compositions (metal oxides, nitrides, and carbides) in the presence of reactive solids or gases. These stable compositions are usually formed as a result of the in-situ reaction [1]. The increase in reaction kinetics during the high-energy milling process occurs through microstructural thinning, repeated cold deformation, and diffraction of particles [2].

When solid particles are micronized, their surface area increases in inverse proportion to the particle size. When the 1cm-sized particle is micronized to a scale of 1µm and 10nm, its specific surface area increases between 10,000 and 1,000,000. The increase in the specific surface area directly affects the dissolution and reaction rates of particles [3]. Most materials produced by mechanochemical synthesis can be produced with its shape having crystallized size on a scale of 1-10 nm. Nanoparticles can be used potentially due to their superior mechanical and physical properties, which allow for many structural applications. Due to the effect of nanoparticles available in the structure of nanostructured materials, their properties such as high hardness, fracture toughness and ductility at low temperatures make them advantageous compared to the equivalent materials in the microstructure. In terms of the development of the nanoparticle surface modifications after the milling process, the potential applications are going on [4].

In recent years, the widespread use of phase composites, which are especially intertwined with mechanochemical technique, together with nano-sized microstructures attracts

* Corresponding author. Tel.: +90-332-582-6000.
E-mail addresses: hakan1440@gmail.com *(H. Gokmese)*, bbostan@konya.edu.tr *(B. Bostan)*, tahaalperyilmaz@atauni.edu.tr *(T.A. Yilmaz)*, ufuktasci@gazi.edu.tr *(U. Tasci)*
ORCID: 0000-0002-5125-9720 *(H. Gokmese)*, 0000-0002-6114-875X *(B.Bostan)*, 0000-0002-4316-6890 *(T.A. Yilmaz)*, 0000-0002-8577-443X *(U.Tasci)*
DOI: 10.35860/iarej.630999

attention [2]. When Alumina's (Al_2O_3) thermal stability and mechanical properties at high temperatures are combined with Magnesium oxide's (MGO) high melting point (2800°C), compressive strength, hardness, and thermodynamic stability and boron carbide's (B_4C) high melting point, excellent rigidity, low specific gravity (2.52 g/cm^3), high elastic modulus, and chemical stability, the properties of the resulting material can be significantly improved [5-10].

Thus, in this study, the synthesizability of nanoparticle B_4C ceramic phase with the mechanochemical method by using B_2O_3-B_4C-C triple system was examined at room temperature. In addition, the powder shape and morphology of synthesized nanoparticle B_4C, the solution of diffraction patterns and determination of planes were identified by TEM.

2. Experiment

The initial components used for the production of nano-B_4C particles by mechanochemical synthesis, which constitute the first phase of experimental studies, were used in the studies in the form of B_2O_3, C and Mg initial powder components, respectively. In the studies, B_2O_3 powder (315μm) obtained from the Eti Mine Enterprise was used as a source of boron. The chemical properties of B_2O_3 powder are stated in Table 1. Carbon powder was used as the carbide-maker starting component and it was obtained from Aldrich Company. The properties of the used carbon powder are shown in Table 2. In order for the B_4C ceramic structure to be synthesized, Mg metal powders obtained from Aldrich Company and used as reactants were used in the studies for the purpose of the reduction of B_2O_3. The properties of Mg powders are also given in Table 3.

Table 1. Chemical properties of the boron oxide powder.

Content	Unit	Value
B_2O_3	%	98.00 min.
SO_4	ppm	500 max.
Cl	ppm	10 max.
Fe	ppm	15 max.

Table 2. Properties of carbon

Vapor pressure	Purity	Shape	Ignition temperature
< 0.1 mmHg (20°C)	99.95%	Powder, ball	842 °F
Specific resistance	Particle size	mp	Density
1375 μΩ-cm (20°C)	2-12 μm	3550 °C (lit.)	2.267 g/cm^3

Table 3. Properties of magnesium

Purity	Shape	Ignition temperature	Specific resistance
≥ 98 %	Powder	950 °F	4.46 μΩ-cm 20°C
Particle size	bp	mp	Density
75 - 200 μm	1090 °C (lit.)	648 °C (lit.)	1.74 g/cm^3

Table 4. Experiment parameters

Experiment	Starting Materials			Total Powder (g)	Reactions	
	B_2O_3	Mg	C			
1	1.074	0.833	0.092	2	$2B_2O_3 + 6Mg + C$ ==> $6MgO + B_4C$	
Milling Parameters (Speks)						Sample Code
Pot Volume (ml)	Ball Diameter (mm)	Ball Weight (g)	Ball Number (Pieces)	Powder / Ball Ratio	Rotation speed (rpm)	Time hours	
50	15.10.5	40	10	1/20	1200	4	S-Mg-3

For the production of nano boron carbide by mechanochemical synthesis, activation processes of B_2O_3, C and Mg powder material starting components were provided in the speks type-milling device. The experiment parameters used for this purpose are given in Table 4.

After the synthesis studies, leaching process (15% HCl) was applied to the powder material mixture in order to remove the impurities such as Fe and MgO which originated from the synthesis environment and the initial components used in the synthesis. Thus, it was aimed to transfer impurities into the prepared solution and to obtain the nano B_4C particles, which were intended to be produced, alone. Size analysis measurements of the synthesized nanoparticle powder mixtures by using speks type milling device were performed. For this purpose, size-analysis-measurements of powder before and after leaching were carried out with the device, which operated with Laser Doppler Electrophoresis technique and made particle measurement with Malvern-Nano-ZS model zeta potential. XRD analysis was performed for determination of the possible compounds in synthesized powder mixtures before and after leaching. XRD studies were conducted with Philips brand X-ray diffractometer device and by using 40kV voltage, 40mA current, and Cu-Kα radiation in the range of $10° < 2\theta < 70°$. Especially after leaching processes, JEOL JEM-1400 Transmission Electron Microscope (TEM) was used for nano-sized microstructural imaging. The images obtained in these studies were recorded with different enlargements having 100kV value and in the range of 500-100/1 in the digital environment. The formula given in the following equation was used for the indexing of the diffraction patterns of synthesized nano-dimensional B_4C particles.

$$d_{(hkl)} = (\lambda \times CL) / R \quad (1)$$

d = Distance between planes (Â), λ = Electron wavelength (Â), CL = Camera length (mm), R = Vectorial distance of the specified spot to the zero axis (mm).

d values were calculated using the equation given above which is also known as camera constant equation (d1, d2, d3 etc.). The d values given for various phases and compounds were examined and indexing of the patterns were performed in terms of the values belonging to the B_4C ceramic phase.

3. Results and Discussions

In speks studies, in terms of magnesiothermic reduction, 4 hours of synthesis was performed with B_2O_3, C and Mg starting components under the study parameters in Table 4 by using reactant Mg metal. XRD analysis of the obtained powder mixture is shown in Figure 1. It is observed that peak values occurring at the end of XRD analysis after 4 hours of synthesis define the initial metallic magnesium, Fe and MgO. Setoudeh et al. showed MGO/ZrB_2 synthesis with the mechanochemical method in ZrO_2, B_2O_3 and Mg ternary system by XRD analysis at the end of 2 hours. They explained that after 15 hours, the transformation began, and nanoparticle ceramic phases could be formed [11]. In the literature reviews conducted on mechanochemical synthesis, the attention is drawn to the type and amount of pollution present during synthesis. It is stated that the powder pollution may be due to the issues such as initial powder impurities, atmosphere, and milling equipment [12]. It can also be stated that this is due to the milling pot and the balls used in synthesizing studies, as well as powder pollution and by-products formed in the process.

It is seen that in XRD analysis after leaching proses, the obtained peak values define the B_4C ceramic phase (Figure 2). Deng et al. explained that in the MGO/B4C powder mixture, which they synthesized mechanochemically, MgO could be removed with a solution of 18% HCl and nanoparticle B_4C could be produced alone [13]. In another study, using XRD analysis, Sharifi and his colleagues showed that the B_4C nanoparticle, which was mechanochemically synthesized alone after leaching, showed similarity to the B_4C in commercial purity produced by the carbothermal method [14]. Thus, the synthesized nanoparticle B_4C ceramic material was also brought out after leaching processes. In addition, MGO and other chemicals with impurities such as Fe were moved to the prepared acid solution, and production of nanoparticle B_4C alone was performed.

The shape and morphological characterization of nanoparticle particles produced using mechanochemical synthesis method and attitudes they had in terms of diffraction pattern studies were revealed after the TEM examinations. After the preparation stages, the examinations were performed by taking the TEM sample on the formvar/carbon grid. In this context, to determine the microstructural behavior of the powder mixture during the TEM examinations, microstructural images from the grid slices on the grid at low magnifications (500) to the high magnifications (300,000) are given in Figure 3. When the microstructure images before the leaching process in Figure 3 are examined, we can say that the microstructure images (a, b) at the low magnification in the grid slice are appropriately dispersed in terms of the powder mixture that was mixed during the sample preparation. However, as it can be understood from microstructure images (e, f) at the high magnifications, intense agglomeration was detected in the powder particles.

From the general distribution of the powder mixture, which was mixed after the preparation phase of the TEM sample, their distribution emerging at high magnifications is shown in Figure 4 by microstructure images. When the general distributions of the powders before leaching and after they were mixed were compared, as shown in Figure 4, it was determined that the general distributions of the mixed powders were more suitable and smaller sizes. The most important element in occurring of this situation is the removal of impurities from the structure by leaching process and the ability to display the nanoparticle B_4C particles alone.

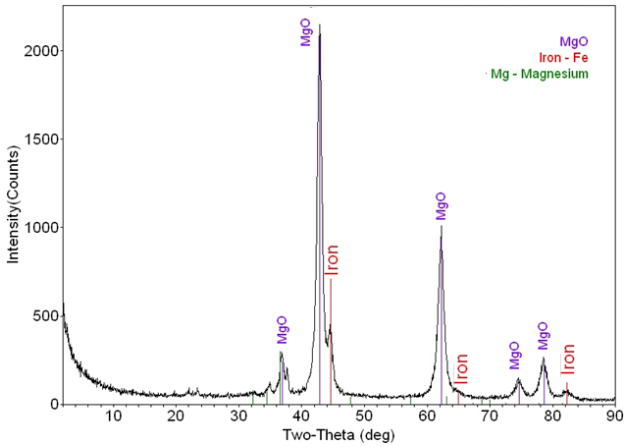

Figure 1. XRD analysis of the powder mixture synthesized for 4 hours (before leaching).

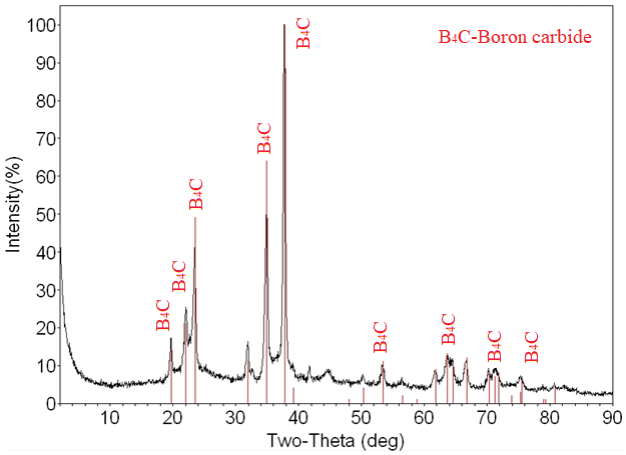

Figure 2. XRD analysis of the powder mixture synthesized for 4 hours (after leaching).

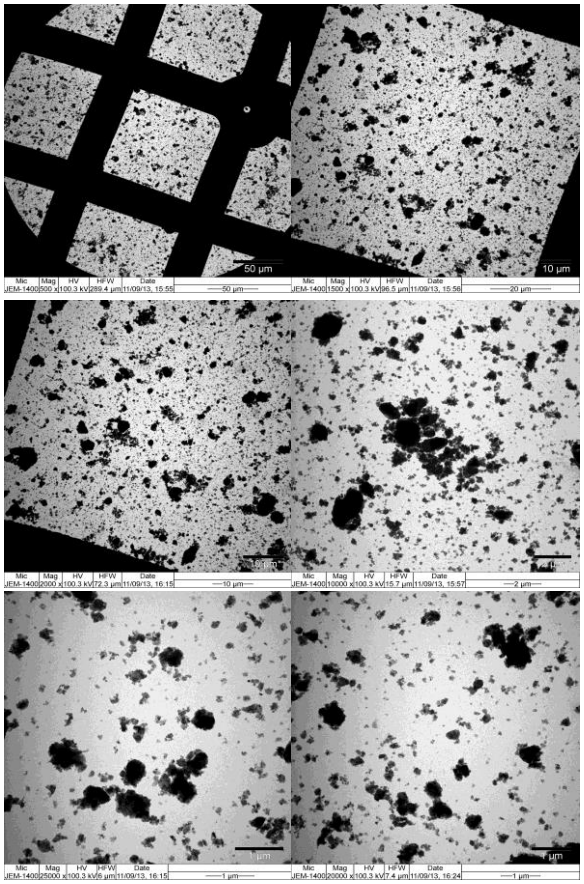

Figure 3. TEM image of powder mixture synthesized for 4 hours (before leaching).

When the microstructure images in Figure 4 are examined, it will be possible to say that the free particles are mostly contained within the structure, rather than the microstructures of B_4C particles prior to leaching operations. When the evaluation is done in terms of the powder shape and morphological aspects, we can say that the powder particles in the equiaxed geometric form are in smaller sizes and that those in polyhedron geometric forms are in larger sizes. It was determined that the agglomerate formation behaviors exhibited by powder particles prior to leaching were also minimized by the leaching process. In the study conducted by Alizadeh and colleagues, the synthesized B_4C particles showed similarity with the TEM image in the equiaxed structure of the nano-sized B_4C particles used as the starting material in composite production [15].

When the microstructure images in Figure 5 were examined, it was possible to see the twin formations exhibited by the B_4C particles after the leaching process in the powder mixture synthesized for 4 hours. In terms of evaluation of the twin formation and TEM examinations; Anselmi and colleagues investigated the effects of synthesis temperature on B_4C structural errors by using spark plasma synthesis method. In their experimental and modeling studies, they focused on the existence of twins [16]. In their other studies, Anselmi and colleagues conducted TEM-oriented simulation studies to analyze the effect of Twin formations, resulting from planar errors, on the X-ray diffraction pattern of B_4C [17].

Li et al. conducted a study on the metal-matrix composite structure of the nano-structured Al 5083/B_4C and deformation twinning in B_4C particles. With TEM studies, they supported the twin formations. They noted that the twin formations in B_4C particles were caused by high shear force and regional high intensity stress forces [18]. The TEM images of the synthesized powder mixture after leaching process also show similarities in terms of twin formation.

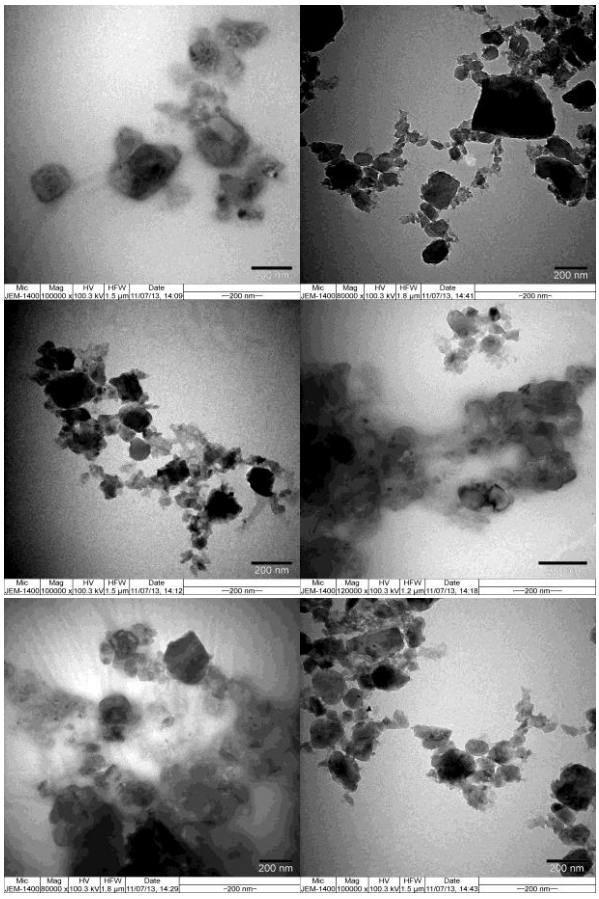

Figure 4. TEM image of the powder mixture synthesized for 4 hours (after leaching).

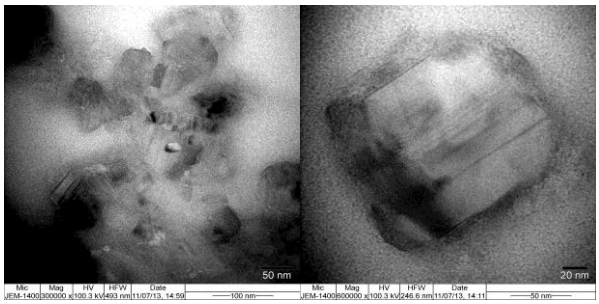

Figure 5. TEM-twin formation of powder mixture synthesized for 4 hours (after leaching).

The size analysis results conducted before and after leaching processes for the powder mixture, which was synthesized at the end of 4 hours when Mg reactant was used, are shown in Figure 6. For the powder-mixture synthesized for 4 hours, the nanoparticle size measurement result conducted before leaching process was determined as Z-average (d.nm) = 405.7 nm. For the powder-mixture synthesized for 4 hours, the sizes of the B_4C particles after the leaching process were measured as Z-average (d.nm) =185.8.

The microstructure images given in Figure 7 show that agglomeration occurred in powders prior to leaching processes. The large values in size analysis measurements are thought to be due to the influence of ceramic phases, which are usually agglomerates. In Figure 7-a, it was determined that powder particles 50 nm and below are present in the TEM image of the powder mixture synthesized for 4 hours before the leaching process. On the other side, in Figure 7-B, it is seen that free particles mostly take part by the effect of the leaching process.

Preparation of TEM sample is very important in TEM examinations. Although it was rare, the negative effects of this condition were encountered during TEM examinations. When the TEM microstructures in Figure 8-a and 8-b were examined, it was observed that the powder mixture could not be distributed well and as a result of this situation, it caused tearing on the grid in the regions where it was densely located. Therefore, TEM sample preparation stages were reviewed and the problems based on deformation that could be in the grid and samples used during the examination were eliminated.

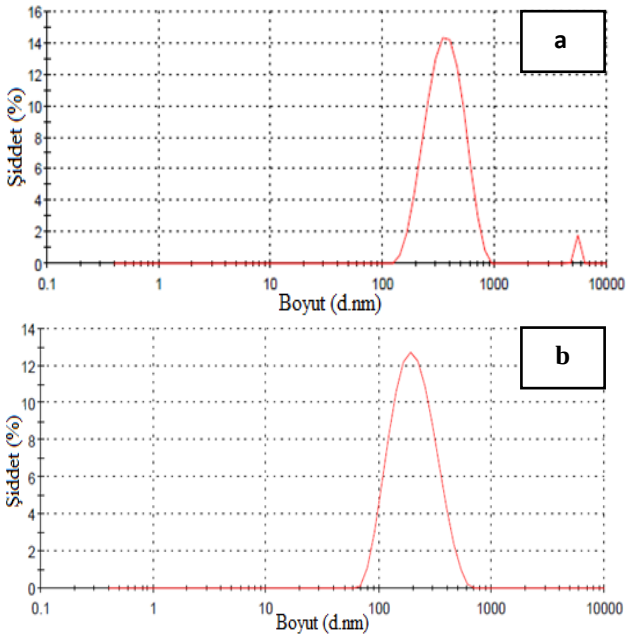

Figure 6. Nanoparticle size analysis of 4-hour synthesized powder mixture; a) Before leaching b) After leaching

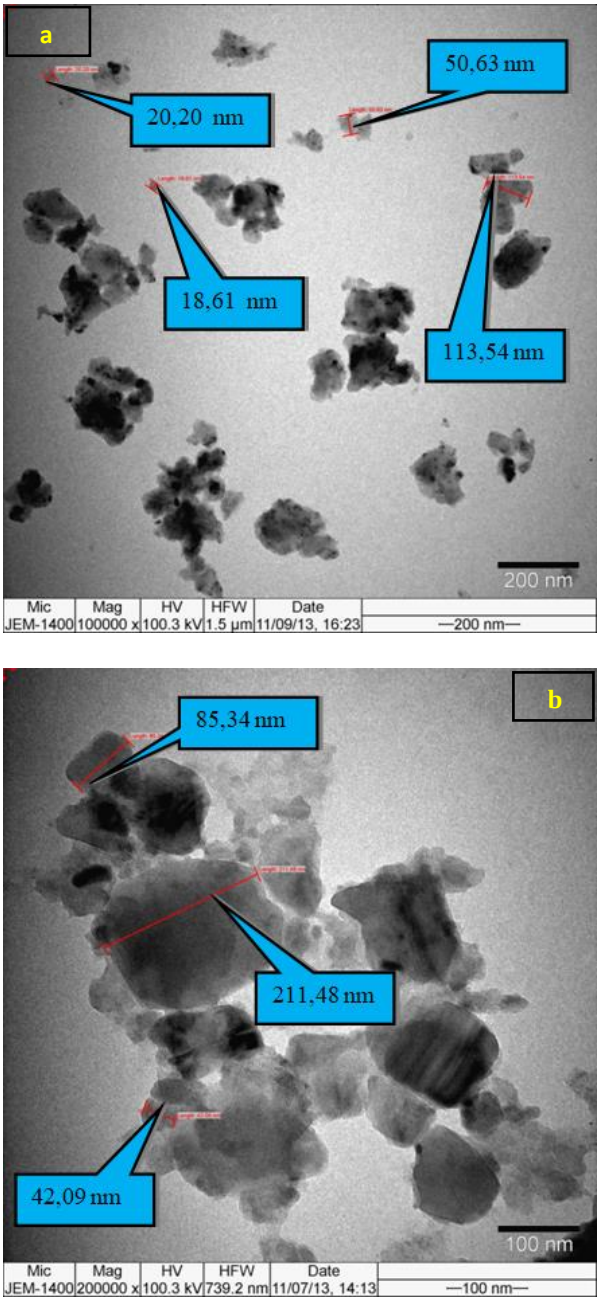

Figure 7. TEM size analysis of powder mixture synthesized for 4 hours: a) before leaching, b) after leaching

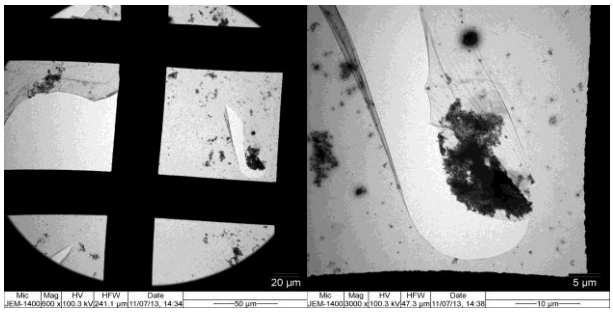

Figure 8. TEM image of the powder mixture synthesized for 4 hours (after leaching).

High-resolution TEM imaging and the examination of the selected-field diffraction pattern were performed only on the powder mixture obtained in nanoparticle size alone after 4-hour synthesis with Mg reactant after the leaching processes (Figure 9). In this context, the high-resolution imaging and selected-field diffraction pattern examination of the nano-sized B_4C particles that were available in the structure after leaching were performed. On its microstructure obtained in TEM image mode over a specific region of the powder mixture synthesized for 4 hours, various B_4C particles in equiaxed, irregular and polyhedral geometric forms are seen. Figure 9 shows the selected area diffraction pattern taken from the same region. When the selected field diffraction pattern was examined, the reflections in the form of spot and ring, which the special orientation of the powder mixture caused, were determined.

In the selected-field diffraction pattern examinations, the agglomerate behavior of the nanoparticle-sized B_4C particles and the fact that they were in coarse particle structures prevented the exact formation of the ring-electron diffraction patterns, one of the TEM indexing techniques, and caused the emerging of discrete ring patterns [14, 19]. At the same time, pattern formations of the amorphous ceramic phase structures that emerged as a result of the mechanochemical synthesis were also found to exist in the structure, mostly in the form of spots and even slightly discrete rings (Figure 9-b).

Jain et al. performed the TEM examinations in their studies conducted on electrolytic production of boron from B_4C particles which they identified as metallic scrap. They demonstrated the discrete and ring-shaped diffraction patterns of boron by examining the selected-field diffraction pattern. They stated that the material was in polycrystalline structure and there were numerous diffraction patterns, and they defined the β-rhombohedral boron structure by diffraction calculations [20]. Li et al. studied the broad twinning attitude in Al-%4Mg-B_4C nanocomposite. With the selected-field diffraction pattern examinations, they mentioned about the formation of discrete ring and spot patterns resulting from the emerging large twin structures [21].

Therefore, as opposed to calculation method via ring proportioning, in the selected-field diffraction pattern examinations, the spot-diffraction-pattern solution method was used in the indexing of B_4C particles. By using the equation given in experimental studies, indexing of B_4C particles was completed. When the selected field diffraction pattern in Figure 9-b was examined, the center spot, on which the reflection occurred, was assumed as a zero (zone) axis and the vector lengths of the reflection spots were calculated according to the center spot.

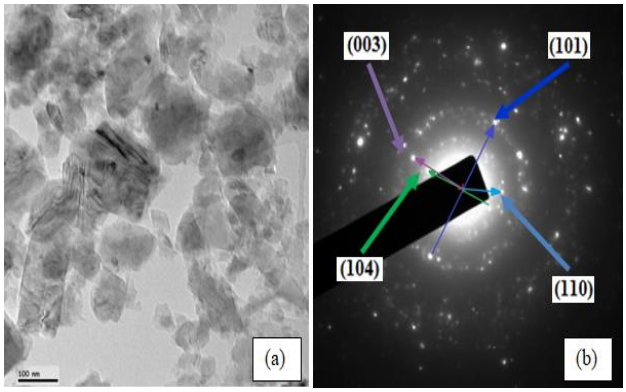

Figure 9. TEM image of powders synthesized for 4 hours (after leaching); a) Bright field image, b) selected-field diffraction pattern.

As a result of the calculations, the coordinates of the spot patterns that made reflection were shown on the images. In line with the vector lengths and camera constant calculations, d values were calculated from diffraction patterns and they were determined as 2,56 – 2,80 – 4,03 – 4,49 Â, respectively. Compared to the diffraction patterns of the B_4C particles, the calculated d values of the reflection spots were found to overlap (Figure 9-b).

4. Conclusions

In this study, related to the synthesis of nanoparticle ceramic B_4C phase after leaching and the production of B_4C particles, which is a high-tech product, at room temperature (as opposed to the chemical methods or high temperatures) by using B_2O_3-Mg-C triple initial powder components via the mechanochemical method, the following conclusions were reached.

- After leaching at the end of 4 hours of synthesis, in XRD analysis, the peaks that define the ceramic phase of nanoparticle B_4C was determined.
- When the TEM microstructure image was examined, it was observed that polyhedron, stick polyhedron and equiaxed B_4C particles were available in the structure.
- As a result of TEM examinations, the presence of twin formations exhibited by B_4C particles was determined.
- When the TEM selected-field diffraction pattern was examined, it was determined that there were many reflections in the form of spot and discrete ring caused by the special orientation of the powder mixture.
- The efficiency of the leaching process made clear the importance of single-phase nano B4C particle synthesis on the reaction activity of the Mg metal.

References

1. Sivasankaran, S., Sivaprasad, K., Narayanasamy, R., Satyanarayana, P.V., *X-ray peak broadening analysis of AA 6061$_{100-x}$–x wt.% Al_2O_3 nanocomposite prepared by mechanical alloying*, Materials Characterization, 2011. **62**: 661-672.
2. Khaghani-Dehaghani M.A., Ebrahimi-Kahrizsangi R., Setoudeh N., Nasiri-Tabrizi B., *Mechanochemical synthesis of Al_2O_3–TiB_2 nanocomposite powder from Al–TiO_2–H_3BO_3 mixture*, Int. Journal of Refractory Metals and Hard Materials, , 2011. **29**: 244–249.
3. Yokoyama, T., *Basic Properties and Measuring Methods of Nanoparticles*, Fundamentals of Nanoparticles, 2013. Chapter 1, 5-10.
4. Castro, C. L. and Mitchell, B. S. *Nanoparticles from Mechanical Attrition*, Functionalization and Surface Treatment of Nanoparticles, 2002. Chapter 1, 1-15.
5. Rahimian, M., Ehsania, N., Parvin, N., Baharvandi, H. R., *The effect of particle size, sintering temperature and sintering time on the properties of Al–Al_2O_3 composites, made by powder metallurgy*, Journal of Materials Processing Technology, 2009. **209**: 5387–5393.
6. Rahimian, M., Parvin, N., Ehsani., N., *The effect of production parameters on microstructure and wear resistance of powder metallurgy Al–Al_2O_3 composite*, Materials and Design, 2011. **32**: 1031–1038.
7. Arslan, G., Kalemtaş, A., Tunçer, E., Yeşilay, S., *Emdirme Sonrası Isıl İşlemlerin B_4C-Al Kompozitlerin Mikro Yapı ve Özelliklerine Etkileri*, Anadolu Üniversitesi Bilim ve Teknoloji Dergisi, 2009. **10**(1): 267-276.
8. Cafri, M., Dilman, H., Dariel, M. P., Frage, N., *Boron carbide/magnesium composites: Processing, microstructure and Properties*, Journal of the European Ceramic Society, 2012. **32**: 3477–3483.
9. Abdizadeh, H., Ebrahimifard, R., Baghchesara, M. A., *Investigation of microstructure and mechanical properties of nano MgO reinforced Al composites manufactured by stir casting and powder metallurgy methods: A comparative study*, Composites: Part B, 2014. **56**: 217–221.
10. Karabulut, H., Çıtak, R., Çinici, H., "*Mekanik Alaşımlama Süresinin Al + % 10 Al_2O_3 Kompozitlerde Eğme Dayanımına Etkisi*", Gazi Üniv. Müh. Mim. Fak. Der., 2013. **28**(3): 635-643.
11. Setoudeh, N., and Welham, N. J., *Formation of zirconium diboride (ZrB_2) by room temperature mechanochemical reaction between ZrO_2, B_2O_3 and Mg*, Journal of Alloys and Compounds, 2006. **420**: 225–228.
12. Suryanarayana, C., *Mechanical alloying and milling*, Progress in Materials Science, 2001, 46, 1-184.
13. Deng, F., Xie, H. Y., Wang L., *Synthesis of submicron B_4C by mechanochemical method*, Materials Letters, 2006. **60**: 1771–1773.
14. Sharifi, E. M., Karimzadeh, F., Enayati, M. H., *Mechanochemical assisted synthesis of B_4C nanoparticles*, Advanced Powder Technology, 2011. **22**: 354–358.
15. Alizadeh, A., Taheri-Nassaj, E., *Mechanical properties and wear behavior of Al–2 wt.% Cu alloy composites reinforced by B_4C nanoparticles and fabricated by mechanical milling and hot extrusion*, Materials Characterization, 2012. **67**: 119-128.
16. Anselmi-Tamburini, U., Munir, Z. A., *Influence of Synthesis Temperature on the Defect Structure of Boron Carbide: Experimental and Modeling Studies*, J. Am. Ceram. Soc**.**, 2005. **88**(6): 1382–1387.
17. Anselmi-Tamburini, U., Ohyanagi, M., and Munir, Z. A., *Modeling Studies of the Effect of Twins on the X-ray Diffraction Patterns of Boron Carbide*, Chem. Mater., 2004. **16**: 4347-4351.
18. Li, Y., Zhao, Y. H., Liu, W., Zhang, Z. H., Vogt, R. G., Lavernia, E. J., Schoenung, J. M., *Deformation twinning in boron carbide particles within nanostructured Al 5083/B_4C metal matrix composites*, Philosophical Magazine, 2010. **90**(6): 783-792.
19. Zheng, R., Hao, X., Yuan, Y., Wang, Z., Ameyama, K., Ma, C., *Effect of high volume fraction of B_4C particles on the microstructure and mechanical properties of aluminum alloy based composites*, Journal of Alloys and Compounds, 2013. **576**: 291–298.
20. Jain, A., Anthonysamy, S., Ghosh, C., Ravindran, T. R., Divakar, R., Mohandas, E., "*Electroextraction of boron from boron carbide scrap*, Materials Characterization, 2013. **84**: 134-141.
21. Li, Y., Lin, Y. J., Xiong, Y. H., Schoenunga, J. M., and Lavernia, E. J., *Extended twinning phenomena in Al–4% Mg alloys/B_4C Nanocomposite*, Scripta Materialia, 2011. **64**: 133–136.